Mansoura Engineering Journal

Volume 48 | Issue 5 Article 12

2023

Effect of Different Nanoparticles SPP Grating on GaAs PIN Photodetector Performance

Nada AbdElaziz
Researcher at Electronics and Communications Engineering Department, Delta Higher Institute for Engineering and Technology, Delta Academy, Mansoura, engnada3112@gmail.com

Eman AbdElhalim
Lecturer at the Electronics and Communications Engineering Department, Mansoura University, Mansoura

Waleed M. Gaballah
Lecturer at Electronics and Communications Engineering Department Mansoura Higher Institution for Engineering and Technology, Egypt

Ahmed S. Samra
Professor at the Electronics and Communications Engineering Department, Mansoura University, Mansoura, Egypt

ORIGINAL STUDY

Effect of Different Nanoparticles Surface Plasmon Polariton Grating on GaAs PIN Photodetector Performance

Nada AbdElaziz [a,*], Eman AbdElhalim [b], Waleed M. Gaballah [c], Ahmed S. Samra [b]

[a] Electronics and Communications Engineering Department, Delta Higher Institute for Engineering and Technology, Delta Academy, Egypt
[b] The Electronics and Communications Engineering Department, Mansoura University, Mansoura, Egypt
[c] Electronics and Communications Engineering Department, Mansoura Higher Institution for Engineering and Technology, Mansoura, Egypt

Abstract

GaAs is currently one of these compound semiconductors' most preferred options for use in photodetector and photovoltaic applications as its increased mobility of electron and states density, in addition to its lower temperature coefficient when compared to silicon [Si]. Different metallic concerning wavelength of light and nanostructures geometry, subwavelength slit structures have plasmonic impacts and could develop a high light intensity region. All of frequencies within the spectrum of interior visible are absorbed inside the bonds, and as a result of their empty states of electron, they can move across the metal by electron transition. In this work, GaAs PIN photodetector with different nanoparticles (NPs) surface plasmon polariton (SPP) such as tungsten (W), palladium (Pd), mercury (Hg), rhodium (Rh), bismuth (Bi), copper (Cu), tin (Sn), gold (Au), and aluminum (Al) are studied, which improve the performance of PIN GaAs modelled photodetector. Internal quantum efficiency (IQE) with the Al SPP grating is 90.76%, whereas IQE of Au SPP grating is 85%, which demonstrated an enhancement of 5.76%. Furthermore, IQE of the proposed GaAs photodetector with no SPP grating is 42.00%, with a total improvement in IQE of 48.76% over the proposed Al SPP grating photodetector. Moreover, the distinctive enhancement in photocurrent and responsivity.

Keywords: GaAs photodetectors, Internal quantum efficiency, Plasmonic photodetectors, SPP grating

1. Introduction

The metals' interaction with the electromagnetic radiation is primarily manifested via the metal's free conduction electrons. Free electron fluctuations are 180° phase out with electric field that is generating in the context of the simplistic Drude model. Extraordinarily high reflectivity is one result of the fact that most metals have a negative dielectric constant at optical frequencies. Additionally, gas of free electrons in the metal at optical frequencies could exhibit oscillations in the volume and surface charge density known as the plasmon polaritons or [plasmons] with different frequencies of resonance as. The plasmons are a defining feature of the metal nanostructures' interaction with light (Ding et al., 2015). Other spectral ranges cannot reliably achieve comparable performance. Due to the fact that the material properties change significantly with frequency, through the Maxwell's equations geometry invariability. This specifically shows that investigations using metal nanostructures at optical frequencies cannot be replicated in model trials using, for example, correspondingly bigger metal designs and microwaves. Similar to the instance of a tiny subwavelength scale particle, if the electron gas is constrained in the three dimensions, the electrons' total displacement according to the particle's

Received 11 February 2023; revised 26 April 2023; accepted 15 May 2023.
Available online 8 November 2023

* Corresponding author at: Researcher at Electronics and Communications Engineering Department, Delta Higher Institute for Engineering and Technology, Delta Academy, Mansoura, Egypt.
E-mail address: engnada3112@gmail.com (N. AbdElaziz).

https://doi.org/10.58491/2735-4202.3053

geometry, a restoring force generated by the positively charged lattice contributes to the growth of particular particle-plasmon resonances. High local charge quantities can occur into particles with the appropriate shape (usually pointed), which is reinforced by much increased optical fields (Brongersma and Shalaev, 2010). Recently, plasmonics or nanoplasmonics has been used to describe the optical phenomena's study related to the electromagnetic response of metals. In particular, this rapid expansion area of nanoscience is related to the optical radiation limitation at subwavelength geometry. Due to the absence of optical concentration, the best method of photodetectors gives the fundamental limitations of device speed and sensitivity (Yousif et al., 2019). Plasmonic field improvement makes use of the coupling between electromagnetic field and oscillations' metal charge. These hybrid charge/external modes of field, known as the plasmon polaritons, could be shrunk to size of an oscillation for metal's charge. Plasmonic devices can function at a deep subwavelength scale because size of that oscillation could be considerably less than corresponding wavelength of light inside a vacuum. When the light's wavelength is consistent with the resonance of the metal nanoparticle, there can be a significant interaction between them. The interaction's degree, the cross-section of scattering, the direction of scattering, and scattering magnitude are all determined by this resonance. The kind of metal, the surroundings, the size and particles' form, and their photonic environment all affect the resonance. According to Fig. 1, there are three main plasmonic processes that might be advantageous for photovoltaics (Daboo et al., 1991). Where (a) light trapping is caused by the front of the solar cell's metal nanoparticles scattering light. Light is primarily scattered, and (b) light trapping is caused by localized surface plasmons' excitation in the metal nanoparticles inserted into the cell, and (c) the light trapping is caused by surface plasmon polaritons' excitation at interface of metal/semiconductor. The first two are based on (localized plasmon polaritons) LPPS, which can provide a local field improvement to increase absorption in the particles' immediate vicinity or employ directed scattering to capture light.

The propagating plasmons serve as the foundation for the third mechanism. The most effective of these processes is the directional scattering strategy, which, if light is intentionally scattered towards the high-refractive index region, may also intentionally provide antireflection qualities.

These detector designs could be fitted to an optical fiber's geometry. According to the losses of the waveguide coupling, grating-type plasmonic photodetectors are often more suitable for attracting signal direct from free space over the type of waveguide photodetectors. Manufacturing benefits, compactness, and photodetection accuracy are all provided by the plasmonic grating. Particularly, grating coupling approach is practical for exciting surface plasmon polaritons on photodetector (Dorodnyy et al., 2018; Takeda et al., 2014). Until now, nanoparticles manufactured of noble metals, typically as Ag and Au, have been investigated thoroughly, because of their efficient plasmonic performance in the visible and infrared region.

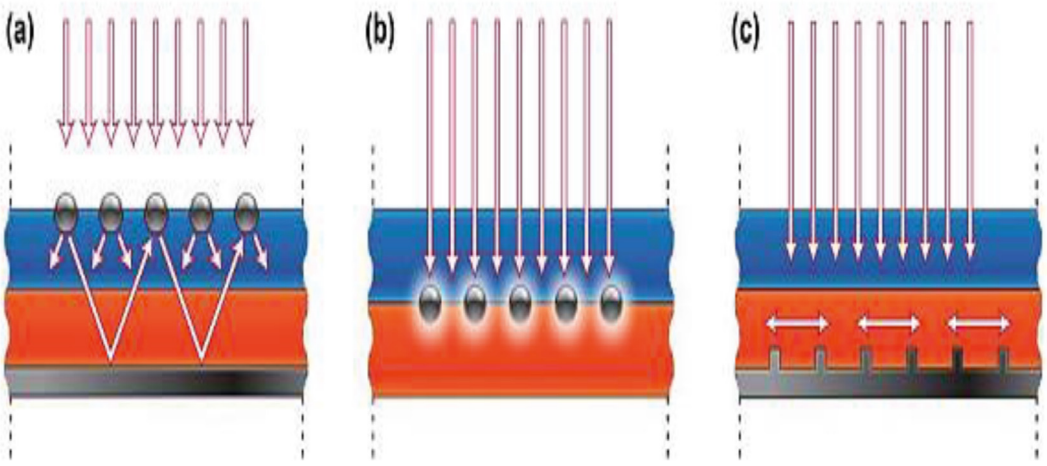

Fig. 1. Plasmonic light trapping structures inside solar cells of thin film. Light is trapped in one of three ways: (a) by scattering from metal (nanoparticles) NPs, which improve the effective light path; (b) by localized surface plasmon excitation that generates a strong near field around the NPs; and (c) by (surface plasmon polaritons) SPPs that propagate laterally along the interface of metal–dielectric (Atwater and Polman, 2011).

Nevertheless, applications in future would need plasmonics extension in the direction of lower wavelengths, particularly in UV ultraviolet (UV) range (Powell and Swan, 1959). Rather than Au and Ag, Al, the most widely available metal in the crust of Earth, can satisfy the need for less investigated.

UV plasmonics. Al is beneficial because of its low intrinsic loss, low screening ($\varepsilon_\infty \approx 1$), the frequency with high plasma (≈15 eV), and appropriate metal oxide semiconductor [CMOS] compatibility (Clark et al., 2018; Cheng et al., 2018; Tan et al., 2014; Shrestha et al., 2014). In this paper, IQE of the modelled GaAs PIN photodetector has been determined. We have taken different nanoparticles' SPP into account in our structure, which achieves a greatly efficient approach to the simulation results. The design demonstrates how light confinement changes when different nanoparticles are used, allowing more photons to access the photodetector. To further explain the effect of the modelled mechanism on enhancing outcomes of the PIN photodetector, the responsivity and photocurrent of this structure are also determined.

The paper remainder are arranged as: Modelled PIN photodetector's structure and parameter values are shown in Section (II). Section (III) provides more information about the SPP mathematical modelling used in this study. Section (IV) describes the outcomes of simulation, and Section (V) represents the research conclusion.

2. Design structure

Modelled GaAs PIN photodetector structure is demonstrated in Fig. 2, which constructed from SPP grating layers made of various nanoparticles such as (copper, bismuth, palladium, mercury, tungsten, rhodium, aluminum, and tin). The active material utilized was GaAs, with 1 [μm] thickness. SPP slices were designed on structure's top, utilizing a silver N connector and a gold P connector to show that the photodiode is being crossed by current when the state of light is produced. Table 1 comprises more statistics about the structure. The design's input majority parameters came from (Yousif et al., 2020). Mesh utilized was free tetrahedral with normal size. Boundary conditions were periodic with continuity sort. The front side of the photodetector is exposed to spectrum light with an intensity for input power of 1000 (W/ m^2) by altering the wavelength of light across range of 450–950 nm. SPP nanograting with Transmission type is crafted to gather the incoming light and pass it to the active layer, then examine their effects on enhancing functionality of the modelled PIN photodiode.

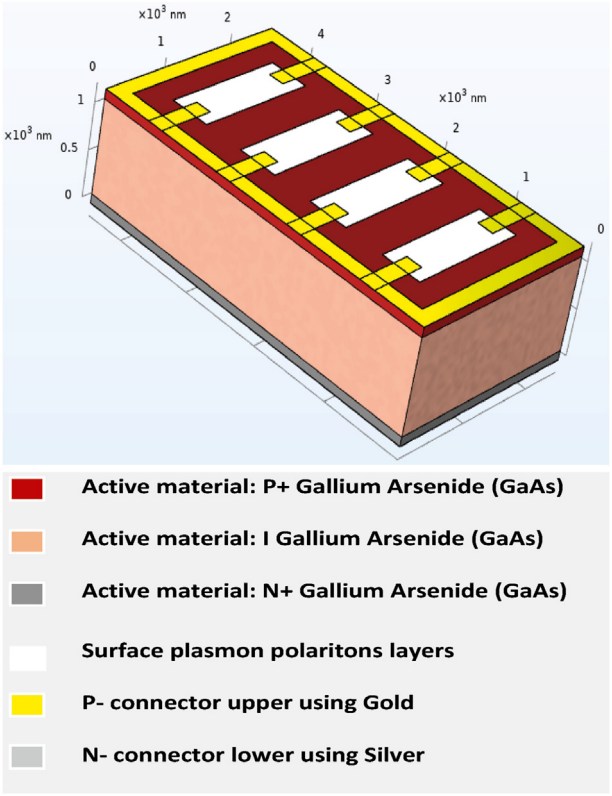

Fig. 2. Design of GaAs PIN modelled photodetector with adding SPP grating composed of various metals nanoparticles such as copper, bismuth, palladium, mercury, tungsten, rhodium, aluminum, and tin.

3. SPP mathematical modelling

The following are some of key characteristics of SPP that will be covered in this section: -

3.1. Excitation of SPP

Via photons or electrons, SPPs could be excited. Through shooting electrons into a metal's bulk,

Table 1. Structure parameters utilized in calculations (Yousif et al., 2020).

Parameters	Values
Intensity of the Input Power	1000 (W/ m^2)
Voltage at (N contact)	2 (V)
Voltage at (P contact)	0 (V)
Refractive Index of GaAs	3.5
The Thickness of Detector	1 (μm)
The Doping of Anode [P+ doping]	1 e^{21} (atom/ cm^3)
The Doping of Cathode [N+ doping]	1 e^{21} [atom/ cm^3]
Doping Anode Thickness	100 (nm)
Doping Cathode thickness	100 (nm)
SPP Slice Width	500 (nm)
Thickness of SPP Slice	3.7 (nm)
The Active Area of GaAs photodetector	4500 (nm) * 2500 (nm)

electron excitation is accomplished (Bashevoy et al., 2006). Energy is transferred to plasma bulk by scattering vector. SPP formation is triggered by one of the components for scattering vector being parallel to surface (Zeng et al., 2013).

The photon must possess same momentum and frequency as the SPP in order to excite it. For a specific frequency, free-space photons, in contrast side, have less momentum than SPPs because of their varied dispersion relations. This momentum disparity prevents a free-space photon coming from air from pairing straight with the SPP. Due to the same purpose that a free-space photon dielectric can not emit energy through the dielectric, the SPP on such a smooth metal surface can not do so (if dielectric is uniform). The transmission loss happened since the total internal reflection is analogous to this mismatch.

3.2. SPP's dispersion relation and fields

The features of the SPP have been determined using equations of Maxwell. Metal/dielectric interaction is indicated as $[z=0]$ plane, thru metal at $[z<0]$, in addition thru dielectric at $[z>0]$ into this system of coordinate. In relation to [x, y, z, and t], the magnetic and electric fields are presented (Raether, 1988; Rohizat et al., 2021; AbdElaziz et al., 2023):

$$E_{x,n}(x,y,z,t)=E_0 e^{ik_x x+ik_{z,n}|z|-i\omega t} \tag{1}$$

$$E_{z,n}(x,y,z,t)=\pm E_0\frac{k_z}{k_{z,n}}e^{ik_z x+ik_{z,n}|z|-i\omega t} \tag{2}$$

$$H_{y,n}(x,y,z,t)=H_0 e^{ik_x x+ik_{z,n}|z|-i\omega t} \tag{3}$$

Where,

(1) Substance kind is signified in $[n]$ (whereas $[n]=1$ when metal at $[\mathbf{Z}<0]$ and $n=2$ when the dielectric at $[\mathbf{Z}>0]$).
(2) $\boldsymbol{\omega}$ specifies angular frequency of wave.
(3) Signs $\pm$ express that $-$ for dielectric,+for metal.
(4) E_z, E_x stand for $[z$ and $x]$ of that electric field vector components, whereas H_y stands for y-component for vector of magnetic field, and residual parameters $[E_y, H_x, H_z]$ are altogether [zero]. That means SPPs are considered TM [transverse magnetic] waves.
(5) [k] refers to wave vector, which is considered complex vector, and components of $[x]$ are considered real, in addition, components of [z] are considered imaginary in the state of the [lossless] SPP, wave oscillates in direction of [x] and tends to decrease exponentially in direction of [z]. For the substances, $[K_x]$ is similar, though $K_{z,1}$ is frequently vary $(K_{z,2})$.
(6) $\frac{H_0}{E_0}=-\frac{\varepsilon_1\,\boldsymbol{\omega}}{K_{z,1}\,C}$, where ε_1 signifies material permittivity [= 1 for metal], in addition, c represents vacuum light speed. and This could be represented as: $\frac{H_0}{E_0}=\frac{\varepsilon_2\boldsymbol{\omega}}{K_{z,2}\,C}$.

Subsequent equations ought to be apprehended for a wave of this form to achieve the Maxwell's equations:

$$\frac{K_{z,1}}{\varepsilon_1}+\frac{K_{z,2}}{\varepsilon_2}=0 \tag{4}$$

$$and\ K_x^2+K_{zn}^2=\varepsilon_n\left(\frac{\omega}{c}\right)^2\ n=[1,2] \tag{5}$$

The wave propagating across surface possesses relation of dispersion, that is gotten via resolving the two equations (4) and (5).

$$K_z=\frac{\omega}{c}\left(\frac{\varepsilon_1\varepsilon_2}{\varepsilon_1+\varepsilon_2}\right)^{1/2} \tag{6}$$

The function of metallic dielectric in an electron gas structure for free electron, that disregards attenuation, is shown as

$$\varepsilon(\omega)=1-\frac{{\omega_p}^2}{\omega^2} \tag{7}$$

where $\boldsymbol{\omega_P}$ stands for bulk plasma frequency, represented by

$$\omega_P=\sqrt{\frac{ne^2}{\varepsilon_0 m^*}} \tag{8}$$

Where n signifies the electron density, e refers to electron charge, m* refers to electron effective mass, and $\boldsymbol{\varepsilon_0}$ stands for free-space permittivity. for the frequencies under plasmon frequency, $\omega<\omega_p$, the values of $\boldsymbol{\varepsilon}$ is negative, equivalent to 0 at $\omega=\omega_p$ and goes positive over the plasmon frequency $\omega>\omega_p$. The surface plasmon wavevector k_{SP} relation is

$$k_x=k_{SP}=\frac{\omega}{c}\sqrt{\frac{\left(\omega^2-\omega_p^2\right)\varepsilon_d}{\omega^2(1+\varepsilon_d)-\omega_p^2}} \tag{9}$$

Where, $\boldsymbol{\varepsilon_d}$ signifies the relative permittivity in dielectric or dielectric constant.

The operational parameters of the PIN photodetector are as follows:

1- IQE [internal quantum efficiency] could be estimated using (Salamin et al., 2018)

$$\mathrm{IQE} = \frac{I_P}{P_{in}} \cdot \frac{hc}{\lambda . e} \tag{10}$$

2- Photocurrent [I_P] could be represented as (Karelits et al., 2018)

$$I_P = IQE.e\left(\frac{P_{opt}}{h.\nu}\right) \tag{11}$$

Where [P_{opt}] signifies optical power, [h] refers to the Planck' constant, and [e] stands for the elementary electron charge. Photocurrent could be defined as an electric current produced by the incident light on the photodetector (Gay et al., 2006).

3- Responsivity (R) could be determined using (Zhao et al., 2020)

$$R = \frac{I_P}{P_{in}} \tag{12}$$

Where $\mathbf{I_P}$ stands for the photocurrent, $\mathbf{P_{in}}$ signifies the input power.

4. Results and discussion

To evaluate the impact of nanoparticles SPP grating on performance of photodetectors, COMSOL Multiphysics platform is utilized to simulate PIN GaAs photodetector and estimate the detector photocurrent, efficiency, responsivity and electric field intensity, then it is added different nanoparticles SPP grating to the surface of the modelled GaAs photodetector and compared between different nanoparticles outcomes to evaluate their impact on modelled photodetector performance.

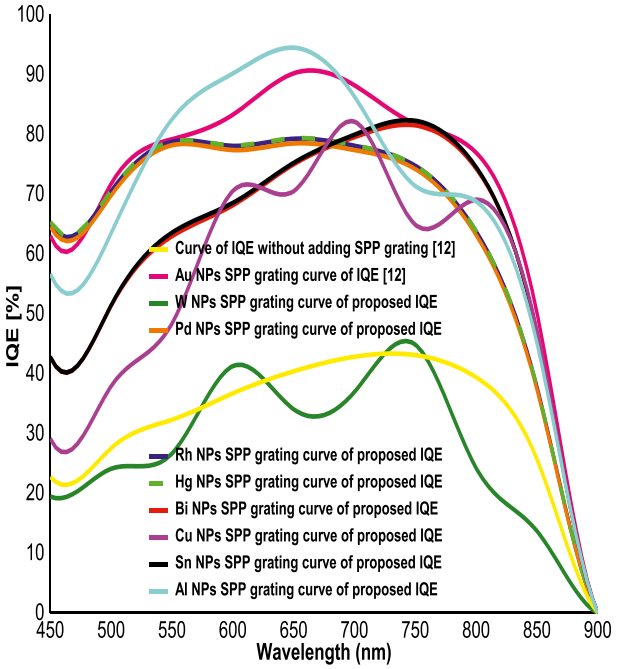

Fig. 4. Modelled PIN photodetector IQE curve with different nanoparticles SPP grating in relation with wavelength.

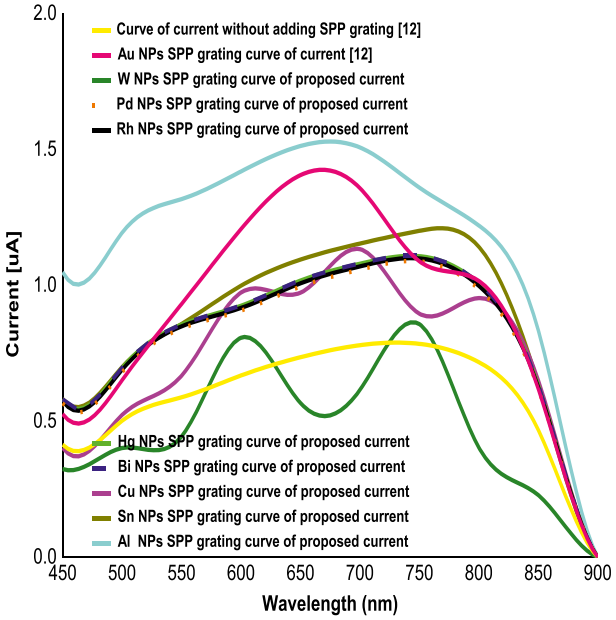

Fig. 3. GaAs PIN proposed photodetector current curve in relation with wavelength [nm] for various nanoparticles SPP grating.

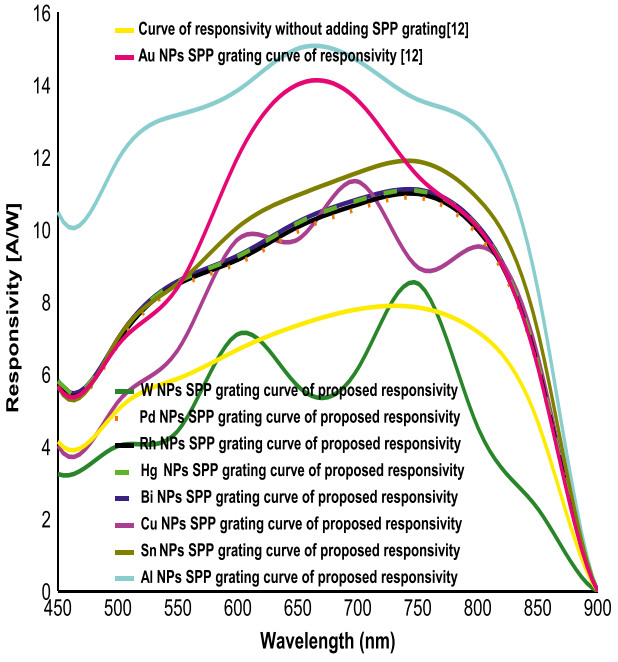

Fig. 5. Proposed PIN GaAs photodetector responsivity curve for wavelengths range with varying nanoparticles SPP grating.

Table 2. GaAs PIN photodetector simulation results values.

Different nanoparticles of SPP	IQE (%)	Photocurrent (μA)	Responsivity (A/W)
Aluminum (Al)	90.76	1.50	15.00
Gold (Au) (Yousif et al., 2020)	85.00	1.40	14.00
Tin (Sn)	82.27	1.17	11.88
Copper (Cu)	82.12	1.13	11.33
Bismuth (Bi)	81.50	1.11	11.10
Rhodium (Rh)	79.35	1.11	11.08
Mercury (Hg)	79.26	1.11	11.07
Palladium (Pd)	77.37	1.09	10.99
Tungsten (W)	44.85	0.86	8.54
Without SPP (Yousif et al., 2020)	42.00	0.75	7.50

4.1. Photocurrent [I_P]

Through a wavelength range from 450 to 900 nm, the photocurrent outcome is assessed. Fig. 3 demonstrates some distinctive attributes that levels of current boost gradually with the wavelength. There is a significant improvement that seems in (Al) SPP grating instance, as photocurrent, within this instance, reached 1.52 μA, which expresses a noticeable improvement over the other nanoparticles that are presented.

Al SPP grating structure demonstrated the best photocurrent outcome of the modelled GaAs photodiode. Because of aluminum possesses material characteristics that allow strong plasmon resonances, encompassing much of the visible region and into ultraviolet [UV] spectrum, due to its low screening ($\varepsilon_\infty \approx 1$) compared to gold ($\varepsilon_\infty \approx 9$). Furthermore, aluminum possesses high density of electron as single atom of aluminum contributes three electrons in comparison with single electron per atom of gold and silver (Becker and Becker, 2012).

4.2. Internal quantum efficiency [IQE]

It is considered an essential component for assessing photodetectors performance. As represented in Fig. 4, the IQE for various nanoparticles SPP grating as tungsten (W), palladium (Pd), mercury (Hg), rhodium (Rh), bismuth (Bi), copper (Cu), tin (Sn), gold (Au), Aluminum (Al), respectively is 44.85%, 77.37%, 79.26%, 79.35%, 81.50%, 82.12%, 82.27%, 85.00% (Yousif et al., 2020), 90.76%. The maximum IQE in this modelled research is for Al nanoparticles SPP grating, at 870 nm wavelength, which achieves an IQE of 90.76% with an overall improvement IQE of 45.91% over W nanoparticles SPP grating and 5.76% over Au nanoparticles SPP grating. IQE for GaAs photodetector with no nanoparticles of SPP grating is 42% (Yousif et al., 2020). IQE improvement of Al SPP grating structure is 48.76% over GaAs photodetector with no SPP grating. Various values for IQE that are stated rely on photocurrent in accordance with equations (10) and (11). Furthermore, they are increased in proportion to it, as the increase in photocurrent, the increase in

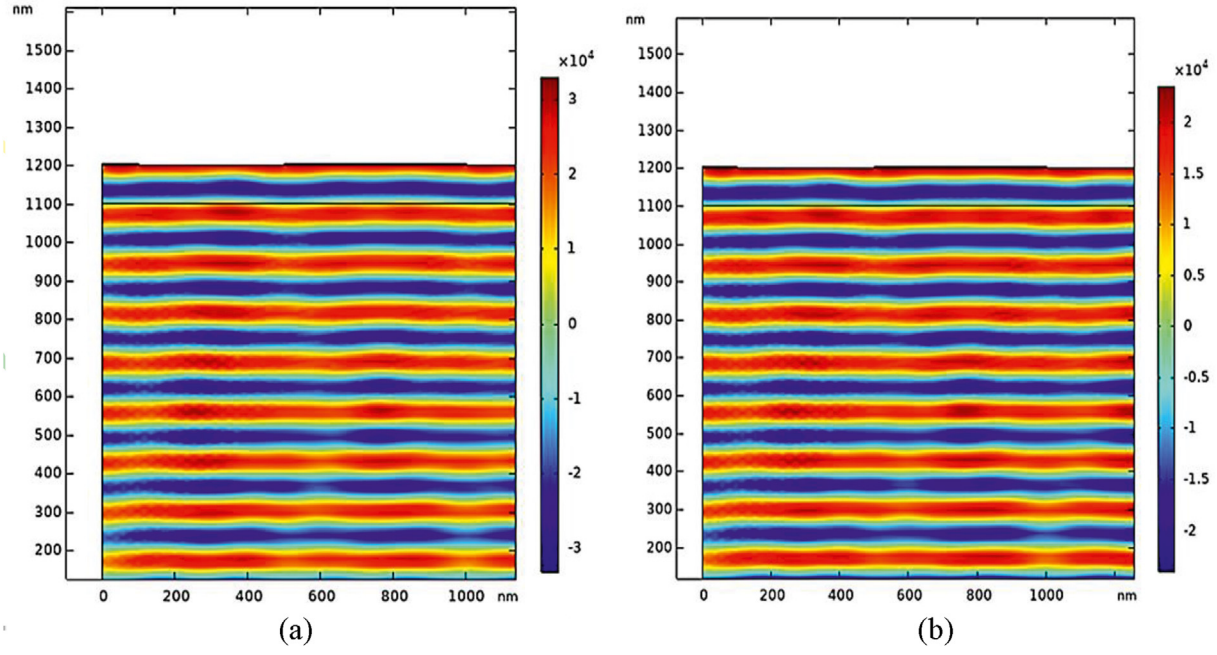

Fig. 6. Proposed GaAs PIN photodiode Electric field intensity at photodetector surface (a) with Al nanoparticles SPP grating (b) without SPP grating.

IQE. It is demonstrated that higher IQE in Al SPP grating case agrees to higher photocurrent value.

4.3. Responsivity (R)

When evaluating performance of photodetectors, an effective critical component to assess is [R] responsivity. These different nanoparticles impact on responsivity is studied also as shown in Fig. 5, it is demonstrated that the maximum responsivity outcome for Al SPP grating reached 15.08 A/W, whereas responsivity of GaAs photodetector with no SPP grating is 7.50 A/W (Yousif et al., 2020). Responsivity is improved by 7.58 A/W in the instance of (Al) SPP grating. This noticeable improvement ratio is increased in proportion to the photocurrent according to equations (11) and (12), which is consequently resulting from an increase in it.

The outcomes of the higher photocurrent, IQE, and responsivity comparison research according to different nanoparticles used are mentioned in Table 2, as demonstrated in the table, Al SPP grating possess the best IQE, indicating the best photodetector performance.

4.4. Electric field intensity

Electric Field Intensity of GaAs PIN proposed photodetector for Al SPP grating and without SPP grating (Yousif et al., 2020) is demonstrated in Fig. 6a and b, respectively, over axis of x and y simulations for distribution of electric field. The light intensity is notable over merging the attributes of SPPs, where intensity of electric field is effectively improved and boosted because incoming light facilitates the electrons in swapping their uniqueness like plasmon polaritons with the aid of Al SPP. Moreover, the intensity of electric field for both Al SPP grating and without SPP grating, more improvement in the Al SPP grating case of modelled GaAs PIN photodetector.

4.5. Conclusion

It is indicated in this proposed study how to design a GaAs photodetector with p-i-n kind utilizing technique of SPP. SPP slices in the proposed structure are nanoparticles of tungsten, palladium, mercury, rhodium, bismuth, gold, copper, aluminum and tin. COMSOL Multiphysics software is utilized to discover electrical and optical influences of SPP grating being added to the surface of photodiode. Various nanoparticles have been designed to realize higher efficiency enhancement over wavelengths range of 450–900 nm. It is indicated that Al SPP grating demonstrates a maximum IQE reached 90.76% at 870 nm wavelength, with an overall improvement in IQE reached 48.76% over proposed p-i-n photodetector with no SPP grating and 5.76% over Au SPP grating structure. Moreover, it enhances the responsivity and photocurrent in comparison with these different other nanoparticles.

Authors contribution

Conception or design of the work: Eman AbdElhalim.

Data collection and tools: Nada AbdElaziz.

Data analysis and interpretation: Nada AbdElaziz.

Funding acquisition: No funding.

Investigation: Nada AbdElaziz, Waleed M. Gaballah.

Methodology: Waleed M. Gaballah.

Project administration: Ahmed S. Samra.

Resources: Nada AbdElaziz, Ahmed S. Samra.

Software: Nada AbdElaziz, Ahmed S. Samra.

Supervision: Ahmed S. Samra.

Drafting the article: Nada AbdElaziz.

Critical revision of the article: Ahmed S. Samra.

Final approval of the version to be published: Ahmed S. Samra.

Conflict of interest

The authors declare that they have no known competing financial interests or personal relationships that could have appeared to influence the work reported in this paper.

References

AbdElaziz, N., Yousif, B., AbdElhalim, E., Gaballah, W.M., Samra, A.S., 2023. Surface plasmonic nano grating for improving GaAs PIN photodetectors performance. Opt. Quant. Electron. 55, 28.

Atwater, H.A., Polman, A., 2011. Plasmonics for improved photovoltaic devices. Mater. Sust. Energy 9 (3), 205–213.

Bashevoy, M.V., Jonsson, F., Krasavin, A.V., Zheludev, N.I., Chen, Y., Stockman, M.I., 2006. Generation of traveling surface plasmon waves by free-electron impact. Nano Lett. 6, 1113–1115.

Becker, J., Becker, J., 2012. Light-scattering and-absorption of nanoparticles. Plasm. Sens. 5–37, ISBN: 978-3-642-31240-3.

Brongersma, M.L., Shalaev, V.M., 2010. The case for plasmonics. Science 328, 440–441.

Cheng, C.W., Liao, Y.J., Liu, C.Y., Wu, B.H., Raja, S.S., Wang, C.Y., Gwo, S., 2018. Epitaxial aluminum-on-sapphire films as a plasmonic material platform for ultraviolet and full visible spectral regions. ACS Photonics 5, 2624–2630.

Clark, B.D., Jacobson, C.R., Lou, M., Yang, J., Zhou, L., Gottheim, S., Halas, N.J., 2018. Aluminum nanorods. Nano Lett. 18, 1234–1240.

Daboo, C., Baird, M.J., Hughes, H.P., Apsley, N., Emeny, M.T., 1991. Improved surface plasmon enhanced photodetection at an Au GaAs Schottky junction using a novel molecular beam epitaxy grown Otto coupling structure. Thin Solid Films 201, 9–27.

Ding, F., Wang, Z., He, S., Shalaev, V.M., Kildishev, A.V., 2015. Broadband high-efficiency half-wave plate: a supercell-based plasmonic metasurface approach. ACS Nano 9, 4111–4119.

Dorodnyy, A., Salamin, Y., Ma, P., Plestina, J.V., Lassaline, N., Mikulik, D., Leuthold, J., 2018. Plasmonic photodetectors. IEEE J. Sel. Top. Quant. Electron. 24, 1–13.

Gay, G., Alloschery, O., De Lesegno, B.V., Weiner, J., Lezec, H.J., 2006. Surface wave generation and propagation on metallic subwavelength structures measured by far-field interferometry. Phys. Rev. Lett. 96, 213901.

Karelits, M., Mandelbaum, Y., Chelly, A., Karsenty, A., 2018. Laser beam scanning using near-field scanning optical microscopy nanoscale silicon-based photodetector. J. Nanophotonics 12, 036002.

Powell, C.J., Swan, J.B., 1959. Origin of the characteristic electron energy losses in aluminum. Phys. Rev. 115, 869.

Raether, H., 1988. Surface plasmons on smooth surfaces. In: Gerhand, Höhler, Niekisch, Ernst A. (Eds.), Surface Plasmons on Smooth and Rough Surfaces and on Gratings. Springer, Berlin, Heidelberg, pp. 4–39.

Rohizat, N.S., Ripain, A.H.A., Lim, C.S., Tan, C.L., Zakaria, R., 2021. Plasmon-enhanced reduced graphene oxide photodetector with monometallic of Au and Ag nanoparticles at VIS–NIR region. Sci. Rep. 11, 1–10.

Salamin, Y., Ma, P., Baeuerle, B., Emboras, A., Fedoryshyn, Y., Heni, W., Leuthold, J., 2018. 100 GHz plasmonic photodetector. ACS Photonics 5, 3291–3297.

Shrestha, V.R., Lee, S.S., Kim, E.S., Choi, D.Y., 2014. Aluminum plasmonics based highly transmissive polarization-independent subtractive color filters exploiting a nanopatch array. Nano Lett. 14, 6672–6678.

Takeda, A., Aihara, T., Fukuhara, M., Ishii, Y., Fukuda, M., 2014. Schottky-type surface plasmon detector with nano-slit grating using enhanced resonant optical transmission. J. Appl. Phys. 116, 084313.

Tan, S.J., Zhang, L., Zhu, D., Goh, X.M., Wang, Y.M., Kumar, K., Yang, J.K., 2014. Plasmonic color palettes for photorealistic printing with aluminum nanostructures. Nano Lett. 14, 4023–4029.

Yousif, B., Abo-Elsoud, M.E.A., Marouf, H., 2019. Triangle grating for enhancement the efficiency in thin film photovoltaic solar cells. Opt. Quant. Electron. 51, 1–11.

Yousif, B., Abo-Elsoud, M.E.A., Marouf, H., 2020. High-performance enhancement of a GaAs photodetector using a plasmonic grating. Plasmonics 15, 1377–1387.

Zeng, S., Yu, X., Law, W.C., Zhang, Y., Hu, R., Dinh, X.Q., Yong, K.T., 2013. Size dependence of Au NP-enhanced surface plasmon resonance based on differential phase measurement. Sensor. Actuator. B Chem. 176, 1128–1133.

Zhao, X., Moeen, M., Toprak, M.S., Wang, G., Luo, J., Ke, X., Radamson, H.H., 2020. Design impact on the performance of Ge PIN photodetectors. J. Mater. Sci. Mater. Electron. 31, 18–25.